



UNIVERSIDAD POLITÉCNICA SALESIANA
SEDE CUENCA
CARRERA DE ELECTRICIDAD

**EVALUACIÓN DE UN SISTEMA DE PUESTA A TIERRA DE LA SUBESTACIÓN EL
BOSQUE**

Trabajo de titulación previo a la obtención del
título de Ingeniero Eléctrico

AUTOR: HENRY BRUNO PACHECO BASTIDAS

TUTOR: ING. HERNÁN PATRICIO GUILLÉN COELLO

Cuenca - Ecuador

2023

CERTIFICADO DE RESPONSABILIDAD Y AUTORÍA DEL TRABAJO DE TITULACIÓN

Yo, Henry Bruno Pacheco Bastidas con documento de identificación N° 0705313351, manifiesto que:

Soy el autor y responsable del presente trabajo; y, autorizo a que sin fines de lucro la Universidad Politécnica Salesiana pueda usar, difundir, reproducir o publicar de manera total o parcial el presente trabajo de titulación.

Cuenca, 5 de octubre del 2023

Atentamente,



Henry Bruno Pacheco Bastidas

0705313351

CERTIFICADO DE CESIÓN DE DERECHOS DE AUTOR DEL TRABAJO DE TITULACIÓN A LA UNIVERSIDAD POLITÉCNICA SALESIANA

Yo, Henry Bruno Pacheco Bastidas con documento de identificación N° 0705313351, expreso mi voluntad y por medio del presente documento cedo a la Universidad Politécnica Salesiana la titularidad sobre los derechos patrimoniales en virtud de que soy autor del Artículo académico: “Evaluación de un sistema de puesta a tierra de la Subestación el Bosque”, el cual ha sido desarrollado para optar por el título de: Ingeniero Eléctrico, en la Universidad Politécnica Salesiana, quedando la Universidad facultada para ejercer plenamente los derechos cedidos anteriormente.

En concordancia con lo manifestado, suscribo este documento en el momento que hago la entrega del trabajo final en formato digital a la Biblioteca de la Universidad Politécnica Salesiana.

Cuenca, 5 de octubre del 2023

Atentamente,



Henry Bruno Pacheco Bastidas

0705313351

CERTIFICADO DE DIRECCIÓN DEL TRABAJO DE TITULACIÓN

Yo, Hernán Patricio Guillén Coello con documento de identificación N°0102063120, docente de la Universidad Politécnica Salesiana, declaro que bajo mi tutoría fue desarrollado el trabajo de titulación: EVALUACIÓN DE UN SISTEMA DE PUESTA A TIERRA DE LA SUBESTACIÓN EL BOSQUE, realizado por Henry Bruno Pacheco Bastidas con documento de identificación N° 0705313351, obteniendo como resultado final el trabajo de titulación bajo la opción Artículo académico que cumple con todos los requisitos determinados por la Universidad Politécnica Salesiana.

Cuenca, 5 de octubre del 2023

Atentamente,



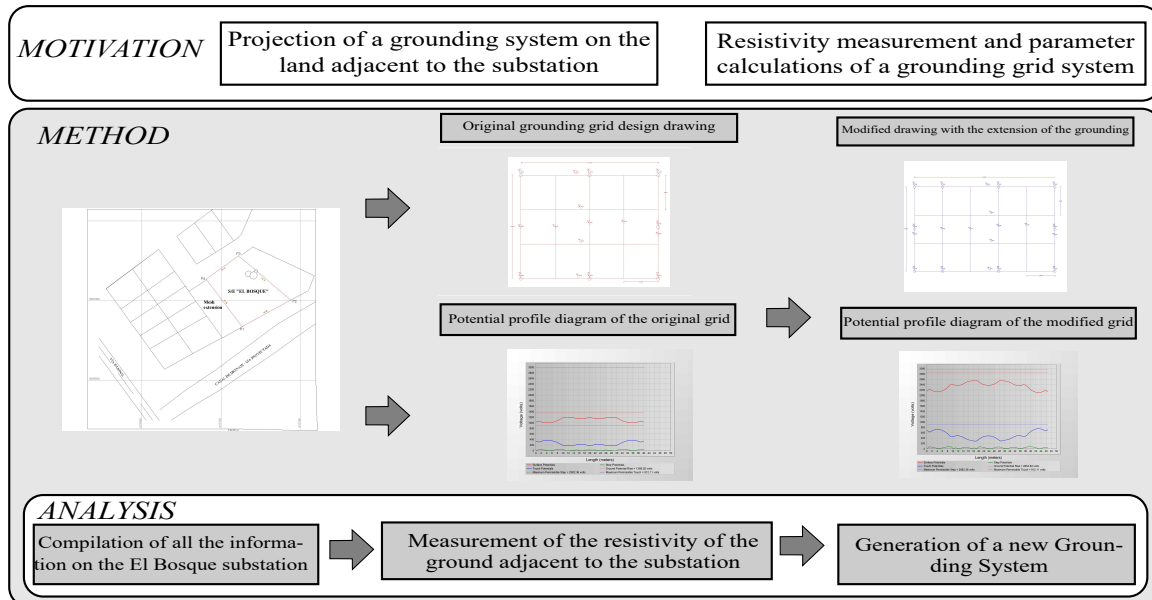
Ing. Hernán Patricio Guillén Coello

0102063120

Graphical Abstract

Evaluation of a grounding system for el bosque substation- Evaluacion de un sistema de puesta a tierra de la Subestacion el Bosque.

Henry Pacheco,Roger Salvatierra,Hernan Guillen



Evaluation of a grounding system for el bosque substation- Evaluacion de un sistema de puesta a tierra de la Subestacion el Bosque.

Henry Pacheco^a, Roger Salvatierra^a and Hernan Guillen^{a,b,*}

^aProgram in Electrical Engineering, Salesian Polytechnic University, Cuenca, Ecuador

^bElectrical Engineer, Salesian Polytechnic University, Cuenca, Ecuador

ARTICLE INFO

Keywords:

Electrical substation
Grounding
Resistivity
CYMGrd
Wenner's

ABSTRACT

The project analyses the effectiveness of the grounding system at the El Bosque substation and determines the feasibility of constructing a new grounding structure on an adjacent site. In summary, various grounding system construction methods, their components and essential formulations for designing a grounding network for medium and high voltage installations are discussed. The aim is to improve the safety of the substation. To do this, the Wenner method is employed with the Geotest Amprobe GP-2 device and the CYMGrd software is used. The study also details how the different resistivities of soils with various physical properties were obtained. The normative reference for this project is IEEE Std. 80-2013.

1. Introduction

A properly designed and constructed earthing system is an essential requirement for the safe operation of an electrical system component, in this case a substation [11]. Its correct performance provides safety and protects people and equipment, counteracting the effects of unwanted voltages or currents, as well as maintaining the integrity of the installations. Its preventive and corrective approach reduces the costs of maintenance, repairs, replacements and loss of operation of machinery due to network phenomena, protecting people's lives [14], [13]. This research work evaluates the SPT of the El Bosque substation under the parameters described in the IEEE 80-2013 standard. The results obtained show whether it satisfies the minimum technical conditions described in the standard, as well as serving as a basis for the design of a new grounded SPT using land adjacent to the substation [30]. For this purpose, the Amprobe GP-2 Geo Test Tellurometer and the CYMGrd software are used to measure the soil resistivity and estimate the resistance of the SPT, respectively. The described equipment is complemented with the [14] standard as the main reference code and the use of updated bibliography [4], [25].

The El Bosque substation (SEB) has a functioning SPT, but it is necessary to assess whether the original design adequately fulfils its protective function. Therefore, this research work seeks to address the needs described above and, using the data obtained, make recommendations to improve the SPT present at the substation [31].

To ensure the safety of both personnel and equipment in a substation, it is essential to implement a grounding network. The adequacy of the proposed design has been

verified by two different approaches: one manual, using the common Microsoft Excel tool, and the other using CYMGRD software. Three key criteria (contact potential, step potential and ground potential rise) have been focused on to assess the suitability of the design. A comparison between these two methodologies was then carried out. The design of the grounding system has been developed according to the standards set by [14], [8].

In recent years, there has been a rapid growth in the demand for electricity. As a result, there has been a steady increase in the construction of substations to meet load requirements. For various technical and safety reasons, it is essential that electrical power installations are earthed, and maintain the lowest possible earthing system resistance to maintain a continuous flow of earth fault current. If the resistance of the grounding system in a substation is high, this could lead to hazardous situations in the vicinity of the substation. This came to the magnitude of the potential difference between earthed structures and various points on the ground during abnormal or fall conditions [5].

Electricity plays a fundamental role in contemporary society. Securing the supply of electricity to communities and addressing space constraints for establishing new substations in urban areas are crucial challenges that the electricity distribution industry must address [26].

Finally, the information obtained will serve as the basis for the conclusions of this research work together with the recommendations derived from the experience at the end of the project.

2. Related Works

An earthing system comprises a set of elements whose purpose is to protect people and equipment from the effect of unwanted electrical currents in a given location. Its mechanism of action is due to the dissipation of unwanted currents to earth through a path of low electrical resistance, providing the current with a route to ground. The implementation of these systems constitutes an effective measure to prevent

*Corresponding authors at Smart Grid Research Group, Salesian Polytechnic University, Quito 010205, Ecuador

**E-mail address:

✉ hpachecob@est.ups.edu.ec (H. Pacheco);

rsalvatierrac@est.ups.edu.ec (R. Salvatierra); hguillen@ups.edu.ec (H. Guillen)

ORCID(s): 0009-0006-1386-5257 (H. Pacheco); 0009-0001-4419-1393 (R. Salvatierra)

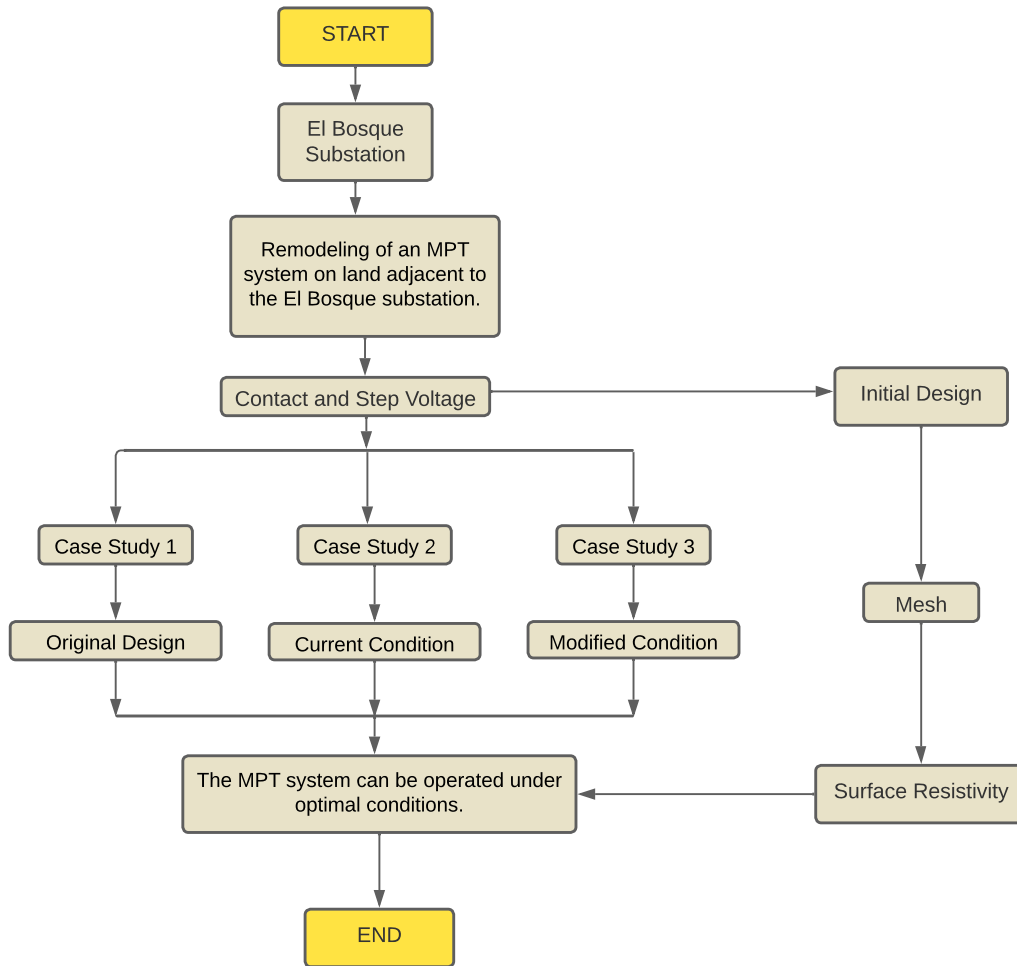


Figure 1: Flow Diagram.

damage and protect people and equipment from electrical phenomena that through disturbances can affect personal integrity or compromise the operation and useful life of equipment or buildings [1]. At the beginning of the 19th century, it was proven that the earth could be used as a current return path for the telegraph network, a single-wire system would be used, with the earth being the element that closed the circuit, allowing the signal to travel to its destination and return [10]. Entering the 20th century, the installation of SPTs began to be permitted under the technical parameters dictated by organisations such as the National Electrical Code and the American Institute of Electrical Engineers. The grounding system is an indispensable requirement for the operation of an electrical substation. Its correct design, construction and operation allow this site to operate safely in the face of phenomena that cause disturbances in the electrical network [16], [9].

Resistivity measurements are made using the tellurometer in order to determine how much the resistivity of the soil varies. Some measurements are made at different points

in the ground and at different distances between the spikes of the equipment. [14] and [11] recommend to perform a measurement and then rotate 90° of the spikes arrangement, forming a sort of cross with respect to the central reference point, so that data will be obtained horizontally and vertically from the ground [11]. The reference standard IEEE Std. 80-2013 establishes the guidelines to obtain the R_g according to the soil conditions to be evaluated and the elements present in the SPT [17]. It is estimated that for a uniform soil model and an MPT composed of horizontal copper conductors and rods vertically embedded in the MPT.

Typically, when a fault occurs in an electrical substation, the resulting current tends to flow through the ground via a set of grounding electrodes. These electrodes generate a resistance to the passage of current, which in turn causes an increase in voltage within the grounding system. This increase in voltage can generate a potential difference which, if it becomes excessive, has the potential to cause damage to equipment and pose a safety hazard to people and animals in the vicinity of the grounded system [27], [20].

Table 1
Nomenclature & Description

Nomenclature	Description	Nomenclature	Description
<i>IEEE</i>	Institute of Electrical and Electronics Engineers	<i>SPT</i>	Grounding system
<i>REP</i>	Equipotential network	<i>CE</i>	Ground conducting wire
<i>MW</i>	Wenner's method	<i>RPT</i>	Grounding resistance
<i>CYMGRD</i>	Applied software for grid simulation	<i>MPT</i>	Grounding grid
<i>GPR</i>	Ground potential rise	<i>DF</i>	Decrement factor
<i>C_s</i>	Surface delayering factor	<i>R</i>	Resistance
<i>PCD</i>	Profile Contour Diagram	<i>ρ</i>	Resistivity
<i>d</i>	distance	<i>SEB</i>	El Bosque Substation

The purposes of a substation grounding system are to ensure the safety of persons in the vicinity of grounded components and to provide pathways for the safe dissipation of electric currents to earth without causing undesirable effects. It is necessary to keep touch and step voltages inside and outside the substation space below established acceptable values, which are determined by the duration of the impact current, the method of protection employed and the accessibility of persons in the substation area [19][28].

This study presents and verifies an extremely simple approach for arranging conductors in the grounding network. This method is based on an arithmetic sequence and guarantees an efficient use of materials, without being restricted in its applicability even in unusual substation surface situations. This is valid for both scenarios with few and multiple conductors in parallel. To corroborate the effectiveness of the method, an analysis of the proposed algorithm is carried out using the Substation Grounding Program CYMGRD [22], [21].

The need to transmit electricity to different regions to meet the demands of society and industry is constantly growing, driving an increase in electricity transmission and distribution activities. This growth in electricity infrastructure also brings with it the need to build new substations to facilitate these processes. These substations play a crucial role in fostering economic development. The purpose of this research is to develop two models of grounding systems. It also seeks to establish the permissible voltage levels for both direct contact and near electrical exposure, and to carry out simulations of both designs using CYMGrd software [15].

3. Problem Formulation and Methodology

The current grounding system at the El Bosque Substation is evaluated to determine if building a new system on a nearby site could improve the protection of the substation. To carry out this evaluation, the Wenner method is used in conjunction with the Amprobe GP-2 Geotest device and CYMGrd software. The reference guidelines used are those established in the IEEE Std. 80-2013 standard. The construction of the El Bosque substation (SEB) is aimed at satisfying the growing energy demand in this region of the country, due to the continuous increase in population and the consequent urban expansion, which is reflected in the construction of

new residential areas, commercial centers, educational institutions, among others. For the resistivity measurement, the tellurometer is used to determine how much the soil resistivity varies. Some measurements are taken at different points of the ground and at different distances between the equipment picks.[14] and [11] recommend taking a measurement and then rotating the spikes 90°, forming a sort of cross with respect to the central reference point, so that data will be obtained horizontally and vertically from the ground [14], [3]. The Wenner method or four-spike method described below is used in this proposal. The IEEE Std. 80-2013 reference standard establishes the guidelines to obtain the R_g according to the soil conditions to be evaluated and the elements present in the grounding system (GPS) [11]. It is estimated that for a uniform soil model and a grounding mesh (GMP) composed of horizontal copper conductors and rods embedded vertically in the GMP, the Schwarz equation can be applied, which establishes four equations to evaluate R_g in a uniform soil and other conditions described in the previous paragraph:

R_1 Ground resistance of the set of horizontal conductors of the mesh, measured in Ω [11].

$$R_1 = \frac{\rho}{\pi L_c} \left[\ln \left(\frac{2L_c}{a'} \right) + \frac{k_1 L_c}{\sqrt{A}} - k_2 \right] \quad (1)$$

R_2 Ground resistance of the set of vertical rods embedded in the mesh, measured in Ω [12].

$$R_2 = \frac{\rho}{2\pi n_R L_R} \left[\ln \left(\frac{4L_R}{b} \right) - 1 + \frac{2k_1 L_R}{\sqrt{A}} (\sqrt{n_R} - 1)^2 \right] \quad (2)$$

R_m Mutual ground resistance between R_1 and R_2 measured in Ω [11].

$$R_m = \frac{\rho}{\pi L_c} \left[\ln \left(\frac{2L_c}{L_R} \right) + \frac{k_1 L_c}{\sqrt{A}} - k_2 + 1 \right] \quad (3)$$

R_g System grounding resistance, measured in Ω [11].

Table 2
Summary of articles related to flaw detection equipment

Author, year	Objectives	Parameters considered				Thematic			
		Voltage	Current	Resistivity	Grounding system	Werner's method	Substations	Earthing resistance	Software Applications
[26], 2022	Grounding assessment of underground substations	✖	✖	✖	✖	-	✖	✖	-
[18], 2019	Influence of grounding wire configuration of traction substation	✖	✖	✖	✖	✖	✖	✖	-
[24], 2021	Creation of software for the planning of grounding systems	✖	✖	✖	✖	✖	✖	✖	✖
[7], 2022	Cost-effective substation grounding design	✖	✖	✖	✖	-	✖	✖	✖
[27], 2021	Optimisation of grounding in high-voltage substations	✖	✖	-	✖	✖	✖	✖	-
[19], 2019	Considerations about Substation Grounding System Design	✖	✖	✖	✖	-	✖	✖	-
[29], 2022	Substation safety assessment for external network failures	✖	✖	✖	✖	-	✖	✖	-
[23], 2019	Digital application for grounding network design calculations	✖	✖	✖	-	✖	-	-	✖
[6], 2022	Analysis of the potential distribution in the grounding network	✖	✖	✖	✖	-	✖	✖	-
[2], 2018	Analysis of substation earthing system performance	✖	✖	✖	✖	-	✖	✖	✖
Present work	New grounding system	✖	✖	✖	✖	✖	✖	✖	✖

$$R_g = \left[\frac{R_1 R_2 - R_m^2}{R_1 + R_2 - 2R_m} \right] \quad (4)$$

- ρ Soil resistivity measured in Ωm .
 L_c Length of the MPT horizontal conductor bundle, measured in m.
 $2a$ Diameter of the horizontal conductor of the MPT, measured in m.
 a' $\sqrt{a * 2h}$ for horizontal conductors buried a depth h, measured in m.
 A Area occupied by the MPT, measured in m^2 .
 L_R MPT rod length, measured in m.
 $2b$ MPT diameter, measured in m.
 n_R Number of MPT rods.
 K_1, K_2 Schwarz coefficients.

The values of k_1 and k_2 are the ratio between the length and width measurements of the MPT and the burial depth h of the MPT, as shown in figure 2.

Curve B: For a depth $h = 0.1\sqrt{A}$

$$Y_B = -0.05x + 1.20 \quad [11]$$

Curve B: For a depth $h = 0.1\sqrt{A}$

$$Y_B = 0.1x + 4.68 \quad [14]$$

Given a surface layer of finite thickness and a bottom layer of infinite depth. This resistivity change is described by the reflection factor equation K, which is for the calculation of R_g for the two-layer soil [14]:

$$K = \frac{(\rho - \rho_S)}{(\rho + \rho_S)} \quad (5)$$

- ρ Resistividad del material superficial, medida en Ωm .
 ρ_S Resistividad de la capa inferior del suelo, medida en Ωm .

The simplified step equation, for meshes with rods along their perimeter or located at the corners, defines a correction factor k_{ii} for irregular current:

$$k_{ii} = 1 \quad (6)$$

For meshes without rods in their perimeter or with few or no rods in the corners, a correction factor k_h is given:

$$k_h = \sqrt{1 + \frac{h}{h_0}} \quad (7)$$

Irregularity factor

$$k_i = 0.644 + 0.148n \quad (8)$$

In our mesh we obtain the following equations to be calculated, where:

$$n_a = \frac{2L_C}{L_p} \quad (9)$$

For "square meshes", "rectangular and square", "L-shaped, rectangular and square" we have the value equal 1

$$n_b = 1, n_c = 1, n_d = 1 \quad (10)$$

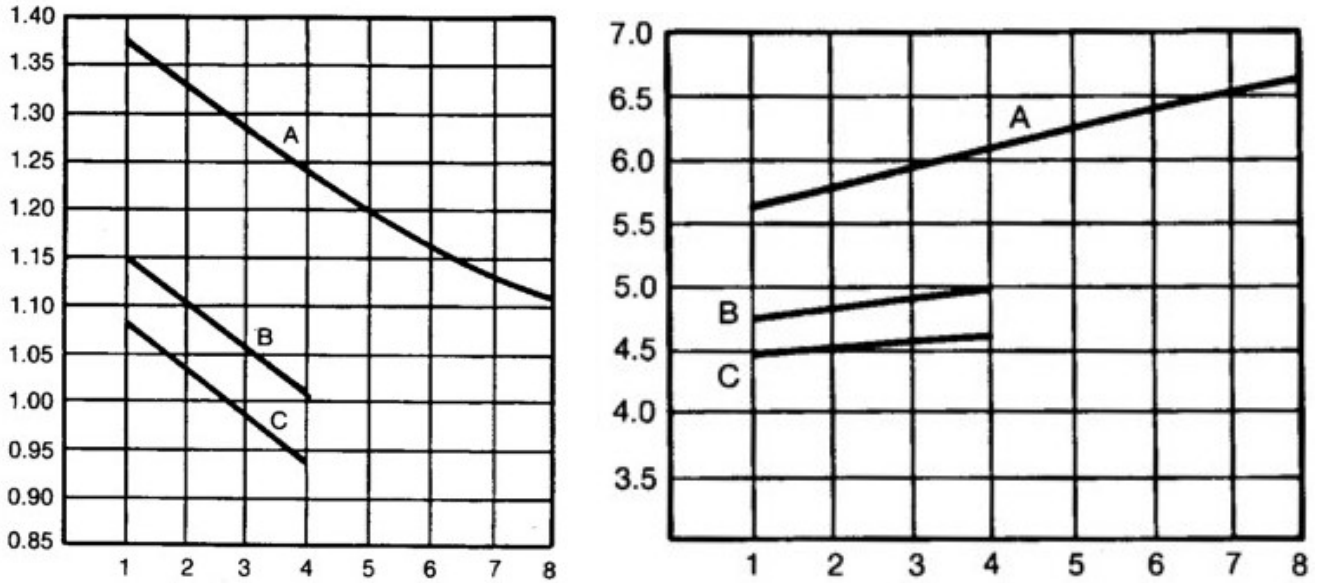


Figure 2: Layout of (a) Length-width ratio curves for coefficient k1 [11] (b) Length-width ratio curves for coefficient k2 [11].

In this case, as we have a rectangular mesh, we apply the following formula:

$$n_b = \sqrt{\frac{L_p}{4\sqrt{A}}} \quad (11)$$

Geometric factor Km of Sverak:

$$K_m = \frac{1}{2\pi} \left[\ln \left[\frac{D^2}{16 * h * d} + \frac{(D + 2h)^2}{8 * D * d} - \frac{h}{4 * d} \right] + \frac{k_{ii}}{k_h} * \ln \left[\frac{8}{\pi(2n - 1)} \right] \right] \quad (12)$$

Effective length of buried conductor (rods + horizontal conductor)

$$L_M = L_C + \left[1.55 + 1.22 \left(\frac{L_r}{\sqrt{L_x^2 + L_y^2}} \right) \right] L_R \quad (13)$$

Mesh voltage:

$$E_m = \frac{\rho * K_m * K_i * I_G}{L_M} \quad (14)$$

- L_p Peripheral length of mesh, measured at m .
- h_0 Take the reference value of 1 as the mesh depth measured in m .
- L_r The length of each MPT rod, measured in m .
- L_R Total length of all MPT rod assemblies, measured in m
- I_G Maximum RMS current flowing between the MPT and the ground, measured at A.

Table 3
Case studies

Case study	Description
Case study 1	Original Design
Case study 2	Current Condition
Case study 3	Condition, Modified

For fault clearance we have the step and touch voltage for a weight of 70 kg, we apply the following equations:

$$E_{step70} = (1000 + 6C_s\rho_s) \left(\frac{0.157}{\sqrt{t_s}} \right) \quad (15)$$

$$E_{touch70} = (1000 + 1.5C_s\rho_s) \left(\frac{0.157}{\sqrt{t_s}} \right) \quad (16)$$

Methodology

Calculations and simulations were then developed for the following substation MPT conditions El Bosque substation, in order to obtain the characteristics to withstand the maximum currents without suffering any damage. Table 3 shows the case studies to be used for each of the following studies.

3.1. Case Study 1

The current grounding grid consists of 248 meters of effective buried conductor, and 8 rods of 2.44 meters buried around the grid.

Table 4 shows the characteristics of case study 1.

Table 4
Characteristics of case study 1.

Characteristics	Value
The fault clearing time	0.5 seconds
The occupied conductor	#2 AWG
The soil resistance	6.43 Ω
The fault current	8119 A

3.1.1. Simulation of the original mesh

The simulation was carried out using finite element analysis with the following characteristics exposed by the IEEE 80-2013 standard, to see if higher current can be supported and how the current mesh behaves.

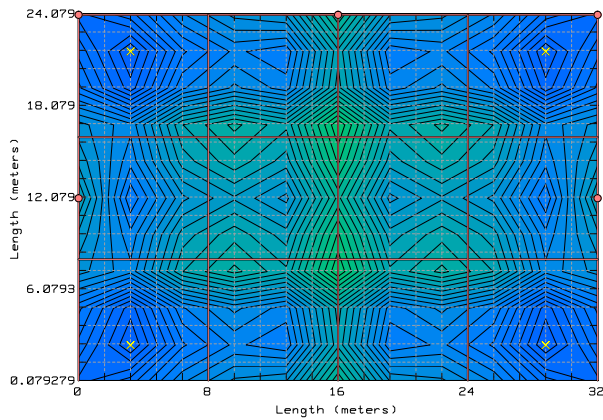


Figure 3: Original design potential contour diagram.

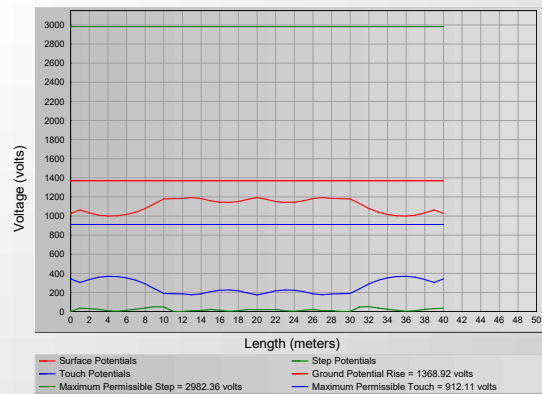


Figure 4: Original design potential profile diagram.

As can be seen, the potential diagram and the contour diagram of the grounding grid have a very favorable

response to the simulation fault exposed in the previous characteristics. Given the calculation analyzed by the soil resistance the mesh presents a resistance of 0.164308 Ω .

3.1.2. Calculation of the parameters of the outer area of the MPT: Original Design.

Simulation at 10 meters

A simulation of the outer mesh spacing at 10 was carried out to check that the step voltage values produced with the current fault current are that the step voltage values produced with the current fault current are within the limits.

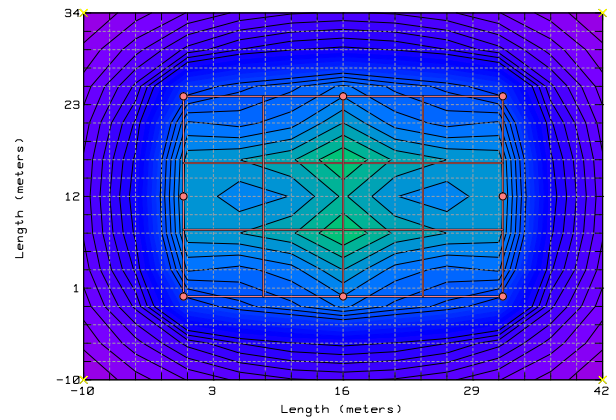


Figure 5: Potential contour diagram of the original design at 10 meters.

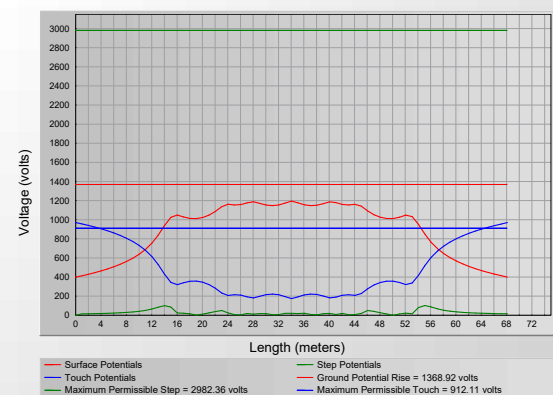


Figure 6: Diagram of potential profile of the original design at 10 meters.

Simulation at 20 meters

A simulation of the outer mesh spacing at 20 was carried out to check that the step voltage values produced with the current fault current are that the step voltage values produced with the current fault current are within the limits.

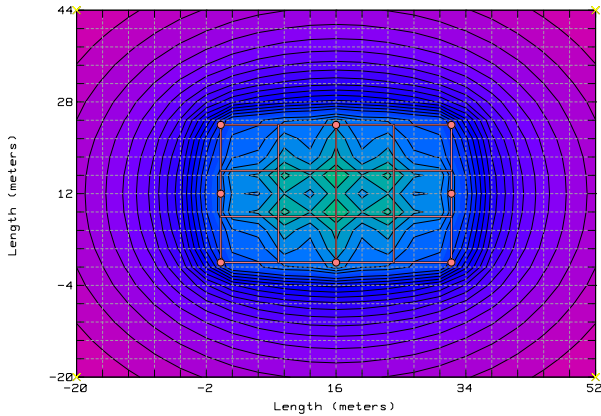


Figure 7: Potential contour diagram of the original design at 20 meters.

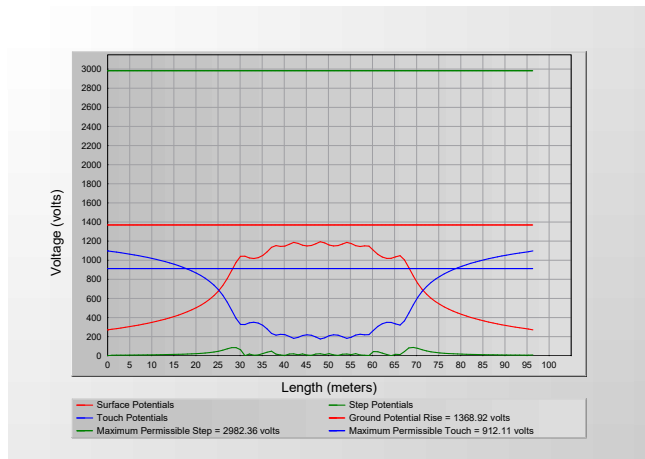


Figure 8: Diagram of potential profile of the original design at 20 meters.

3.2. Case Study 2

3.2.1. Modified MPT resistivity measurements

The soil resistivity value of the EL BOSQUE substation, in the city of Machala, was met through measurements using the measurement tool: Amprobe GP-2 Geo Test, is composed of four stakes and four conductors, linked to the stakes, 20 meters long, obtaining as a value the electrical resistance of the ground, to subsequently obtain the resistivity of the soil. In this table you can see the results of the measurements taken and which site they are closest to as a reference point. At each point measured, 3 measurements were obtained in

order to avoid measurement error. The tellurometer rods were placed at a distance of 1 meter, 2 meters and 4 meters from each other. vertical and horizontal, for the resolution of the soil resistivity analysis the uniform soil criterion supported by IEEE 80-2013 was applied.

For the soil measurement the uniform soil model shown in the table 5.

Being a place where the population is constantly growing, the substation will have to grow, as a consequence more land will be needed, it would be possible to simply change the level of power subtransmission, but it would entail greater economic consequences because it would have to modify the entire voltage level of subtransmission, we analyze how much can increase the substation according to the most optimal land available around the substation.

Given the measurement is said place.

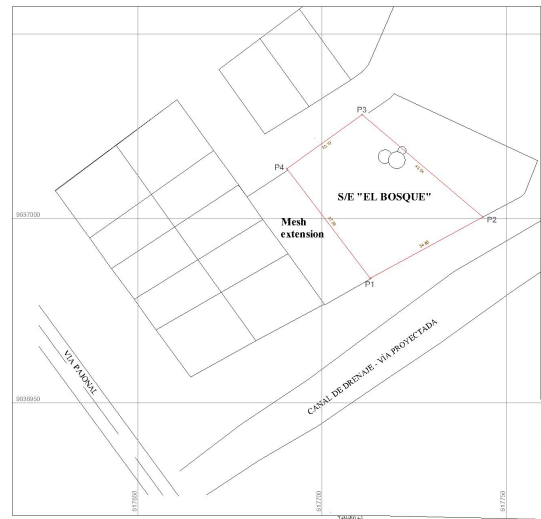


Figure 9: El Bosque substation plan with enlarged grid

The reflection coefficient by applying equation 5.

$$k = 0.9934$$

Corrective factor K_{ii} according to Equation 6

$$K_{ii} = 1$$

Factor k_h under equation 7.

$$k_h = \sqrt{1 + \frac{0.8}{1}} = 1.3416$$

We have the values n_a , n_b , n_c , n_d and n by applying equations 9, 10 and 11 :

$$n_a = \frac{2 \times 248}{32 + 24} = 8.8571$$

$$n_b = \sqrt{\frac{112}{4 \times \sqrt{32 \times 24}}} = 1.005$$

$$n_c = 1$$

Table 5

Measurement of the resistivity of the continuous ground of the "El bosque" substation.

Substation soil resistivity measurements "EL Bosque"			Average
1 m	2 m	4 m	
10,13	9,46	10,36	9,98333333
9,35	10,85	9,58	9,92666667
8,3	15,23	10,33	12,78
8,7	14,07	9,1	11,585
7,68	9,09	10,19	8,98666667
10,56	9,56	10,8	10,30666667
8,56	8,82	9,56	8,98
5,84	6,37	7,3	6,50333333
15,04	7,09	6,7	9,61
Average Total			9,8512963

$$n_d = 1$$

$$n = 8.85711 \times 1.005 \times 1 \times 1 = 8.9028$$

The irregularity factor k_i , under the expression 8:

$$k_i = 0.644 + 0.148 \times 8.9028 = 1.9616$$

The geometric factor K_m of Sverak is, according to equation 12:

$$K_m = 0.75$$

Calculation of L_M and I_G by applying expressions 13 and 14

$$L_M = 279.7$$

$$I_G = 17581.259770$$

Then, the current mesh can support a maximum current of 17581.259770 A.

3.2.2. Simulation of the actual mesh

The simulation was performed using finite element analysis with the characteristics set forth by the IEEE 80-2013 standard.

3.2.3. Calculation of the parameters of the outer area of the MPT: Current Mesh.

Simulation at 10 meters

A simulation of the external environment of the grounded grid structure was carried out at distances of 10 metres. The purpose of the simulation was to verify if the step voltage levels generated by the actual fault current to obtain as a result, if it is within the previously predefined thresholds.

Simulation at 20 meters

A simulation of the external environment of the grounded grid structure was carried out at distances of 20 metres. The purpose of the simulation was to verify if the step voltage levels generated by the actual fault current to obtain as a result, if it is within the previously predefined thresholds.

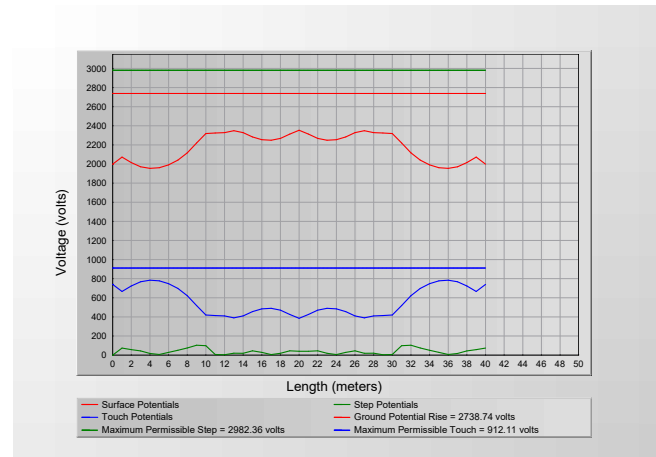


Figure 10: Diagram of the potential profile of the current grid.

3.3. Case Study 3

Step and touch voltage, we have for $t = 0.5s$ fault clearance and for a weight of 70 kg equations 15 and 16 apply:

$$E_{paso} = 2980V$$

$$E_{toque} = 911V$$

The coefficients K_1 and K_2 are calculated, in addition to the resistances R_1 , R_2 , R_m and R_g are calculated in order to obtain the resistance of the mesh, applying expressions 1,2,3 and 4 respectively.

$$K1 = 1.1166$$

$$K2 = 4.8466$$

$$R1 = 0.1736\Omega$$

$$R2 = 0.41208\Omega$$

$$Rm = 0.1299\Omega$$

$$Rg = 0.167734\Omega$$

As we know the mesh is perfectly able to withstand the fault current, so in this section we analyze how much more

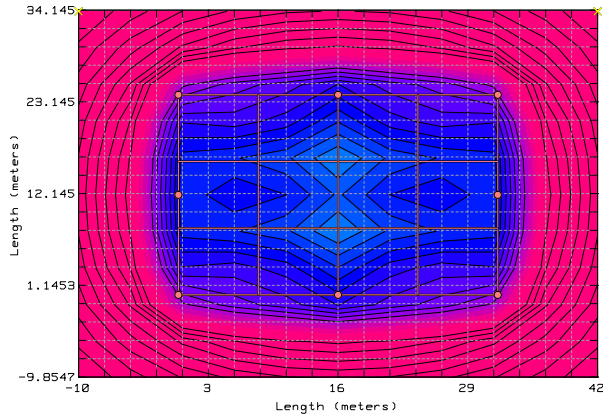


Figure 11: Contour plot of current mesh potential at 10 meters

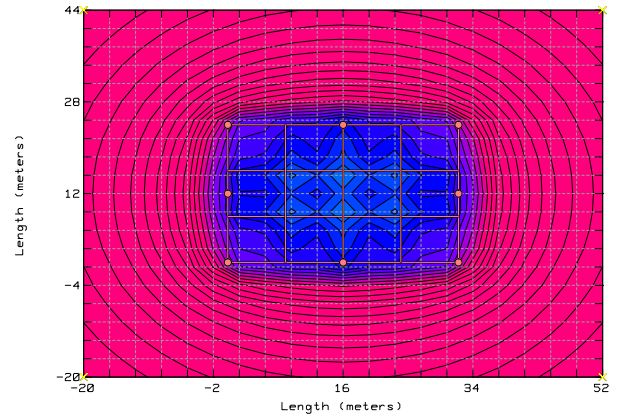


Figure 13: Contour plot of current mesh potential at 20 meters.

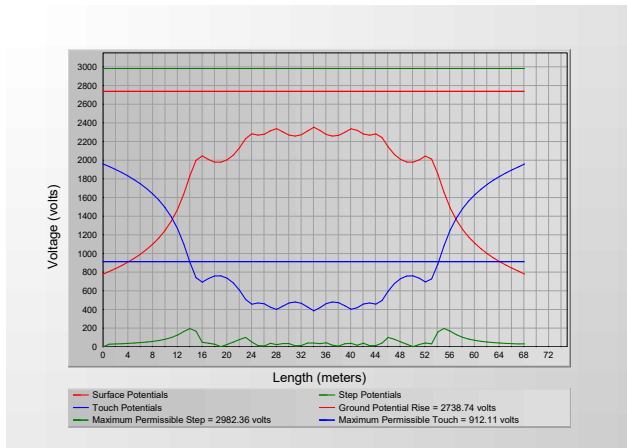


Figure 12: Diagram of current mesh potential profile at 10 meters

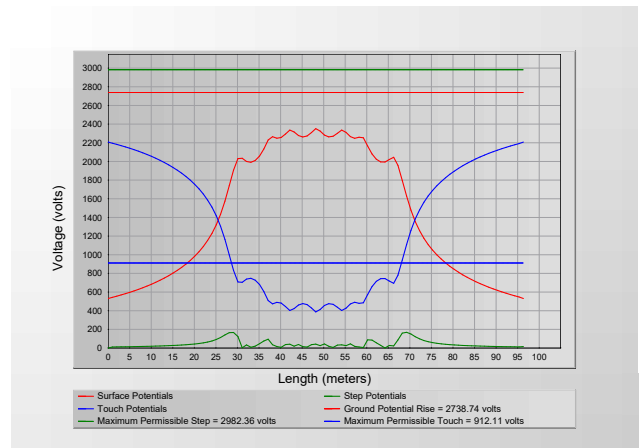


Figure 14: Diagram of current mesh potential profile at 20 meters

the mesh is able to withstand, in case you want to increase its power so also its short circuit current can increase or decrease according to its configuration, usually its value increases by the transformers in parallel. In general, the most important aspect is the touch voltage or mesh potential, which determines the effective performance of the mesh. We obtain our parameter calculation data to obtain our modified mesh by applying the following equations 6, 7, 8, 9, 10, 11, 12, 13 and 14:

$$\begin{aligned}
 K_{ii} &= 1 \\
 K_h &= 1.3416 \\
 n_a &= 4.75 \\
 n_b &= 2 \\
 n_c &= 1 \\
 n_d &= 1 \\
 n &= 9.5 \\
 K_i &= 2.05 \\
 K_m &= 0.745763
 \end{aligned}$$

$$\begin{aligned}
 L_m &= 343.3777 \\
 I_G &= 20770.4425A
 \end{aligned}$$

Once the fault current at which the mesh can operate without any problem has been calculated, it is preferable to analyze the potential profiles of the mesh in areas of interest according to the last chapter of the IEEE 80-2013 standard.

3.3.1. MODIFIED MESH SIMULATION

As for the potential contour, it remains in adequate margin although it is not evenly distributed even though the mesh is symmetrical.

As can be seen in the graph of the potential profiles, the mesh can operate well with the calculated short-circuit current.

3.3.2. Calculation of the parameters of the outer area of the MPT: Modified Mesh.

Simulation at 10 meters

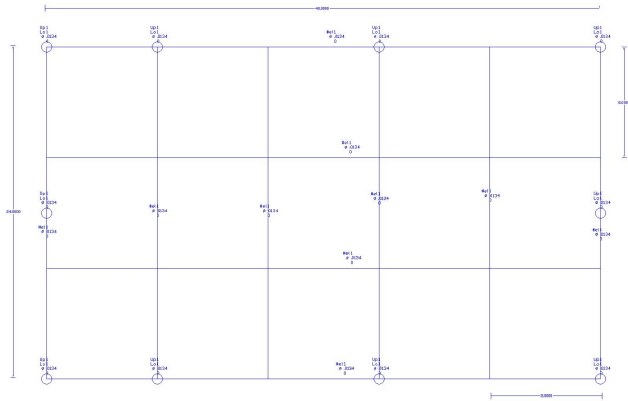


Figure 15: Structured plan of the MPT

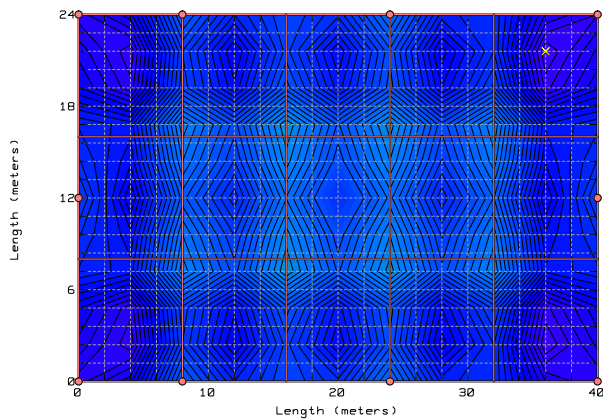


Figure 16: Modified mesh potential contour diagram.

A simulation of the outer mesh spacing at 10 was carried out to check that the step voltage values produced with the current fault current are that the step voltage values produced with the current fault current are within the limits.

Simulation at 20 meters

A simulation of the outer mesh spacing at 20 was carried out to check that the step voltage values produced with the current fault current are that the step voltage values produced with the current fault current are within the limits.

3.3.3. Summary of results

As analysis of results, we have the present table 6 that shows the most fundamental results of the conditions of the MPT of the substation El Bosque. As is known, the main objective is to previously know how much the size of the substation can be increased according to the grounding

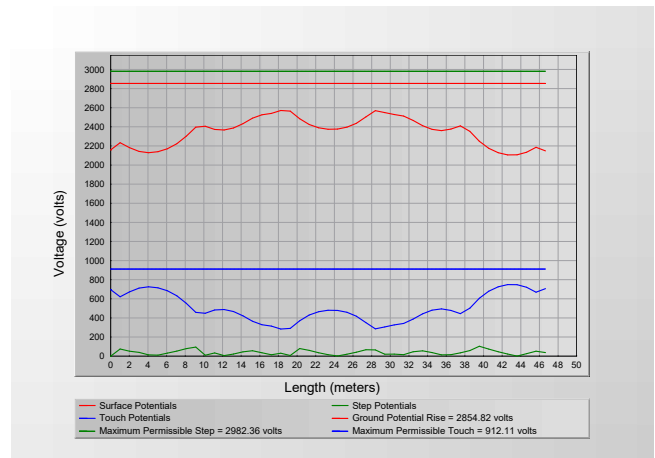


Figure 17: Modified mesh potential profile diagram.

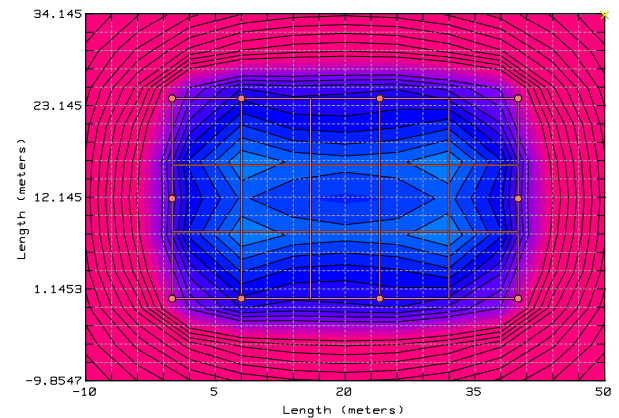


Figure 18: Contour plot of modified mesh potential at 10 meters.

mesh with the available land around it, through the analysis of elements, infinite mesh configurations can be made, so the symmetrical configuration already applied is used, generating 3 cases, the first consists of the current substation without any change, the second the current mesh with the maximum current it can support given the configuration, and finally modifying the mesh taking advantage of the available land around it. In which the modified grid has the best characteristics, due to its greater extension of land for its implementation, allowing the fault current to be dissipated more easily to earth.

4. Discussion

When the SEB's SPT was built], with the aim of satisfying society's energy needs, the aim is to evaluate the system built, so that the results obtained can be used to determine whether the results of the study favour the execution of work

Table 6
Table of value of the Case Studies.

Potential profile diagram							
PARAMETERS		ORIGINAL MESH		CURRENT MESH		MODIFIED MESH	
DISTANCES		10 m	20 m	10 m	20 m	10 m	20 m
Threshold levels of Contact Potential (Volts)	Earth Potential Rise	1368,92	1368,92	2738,74	2738,74	2854,82	2854,82
	Maximum Step Voltage	2982,36	2982,36	2982,36	2982,36	2982,36	2982,36
	Maximum contact voltage	912,11	912,11	912,11	912,11	912,11	912,11
Maximum Potential Points (Volts)	Surface Potentials	1194,1	1193,49	2585,77	2585,77	2837,12	2855,47
	Passing Potentials	101,28	86,79	219,31	219,31	153,34	160,88
	Contact Potentials	970,149	1097,35	2100,8	2100,8	2146,14	2436,52
Mesh Analysis (Ohms)	Calculated Earth Resistance	0,164308	0,164308	0,164308	0,164308	0,145191	0,145191
	Equivalent Impedance	0,164305	0,164305	0,164305	0,164305	0,145189	0,145189
Output results	Decreasing factor	1,02618	1,02618	1,02618	1,02618	1,02618	1,02618
	Reduction factor	0,680674	0,680674	0,680674	0,680674	0,690674	0,690674

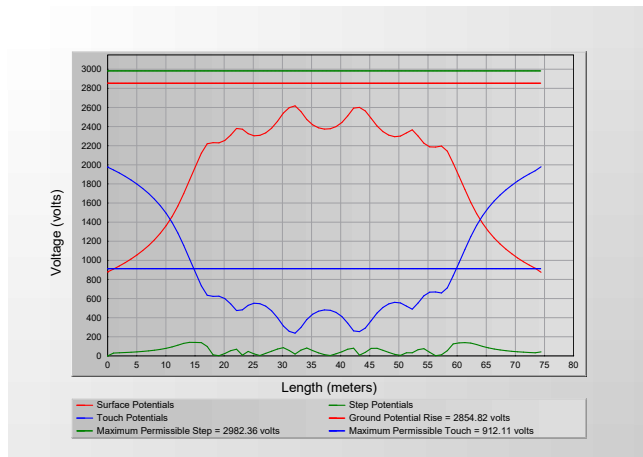


Figure 19: Modified mesh potential profile diagram at 10 meters.

to improve the SPT. Based on the results obtained in Table 6 of the case studies: Case 1, Case 2, Case 3 of the potential profile diagram, results in different parameters are acquired.

The El Bosque substation was built with the aim of supplying the energy demand in this part of the country due to the constant population growth, manifested by the urban expansion, which is manifested by the construction of new citadels, commercial centres, educational institutions, etc. This growth implies a greater need for energy in the area.

The grounding system (GPS) allows both electrical equipment and non-electrical elements to be connected

to earth or a common metallic reference structure, which also has a connection to earth. This grouping contains the grounding (PT) and a set of equipotential cables which, under normal site operating conditions, do not normally carry electrical current. Grounding (PT) is defined as the set of equipotential bonding conductors electrically connected to the ground or to a common metallic reference structure, which is responsible for distributing the electrical fault currents to the ground or earth. This group includes electrodes (rods, conductors, plates or meshes), connections (exothermic welding or compression connector) and buried cables.

5. Conclusions

- The mesh potential and the step potential tend to reduce amplitude to 66% due to the effect of the voltage drop due to the resistance of the ground, on the other hand the touch voltage tends to 45% to be dangerous outside the substation, this is due to the fact that the mesh sends the currents to earth, the elements that are buried around the mesh must be protected by a cathodic protection, otherwise the system will be subjected to constant discharges generated in a substation causing oxidation in them.
- It is indisputable that all metallic objects, such as busbars and transformer casings, that are not grounded to earth around the substation do not have a high touch voltage at 912. 11 V, because it could be observed in the simulations that the touch voltage is at a dangerous level outside the substation for the

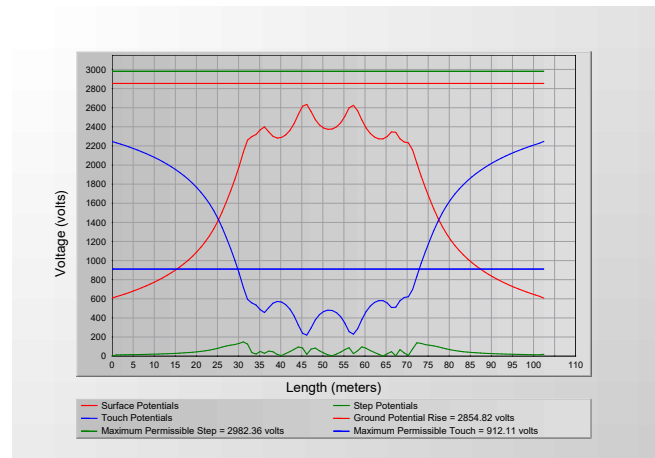
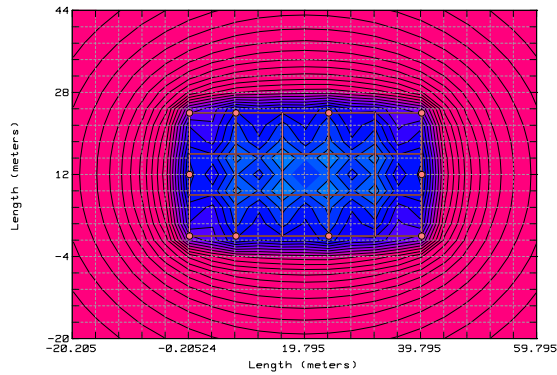


Figure 20: Layout of (a) Contour plot of modified mesh potential at 20 meters. (b) Modified mesh potential profile diagram at 20 meters.

personnel, in general the regulations such as the NEC and the IEE80-2013 standard, recommend that if the metallic elements are more than 5 meters outside the substation they do not need to be grounded, with the exception that if the metallic object is located under the transmission lines, it is not necessary to ground it transmission lines. It is therefore important to analyse at what distance it is advisable not to ground metallic objects depending on the characteristics of the substation, such as short-circuit current, areas available for the substation and design of the mesh and level of ground resistance.

- Given the analysis of the regulations, the level of ground resistance directly affects the sulphation of the conductors, especially if the conductor used is aluminium; having a lower resistance to 9.8512 ohms as in the case of the El Bosque substation, the conductors present a more accelerated sulphation, so the lower the resistance, the greater the amount of PH in the ground, a conductor such as copper is placed with a larger dimension, especially due to the recommendations of Std. IEEE-80-2013 and Chap 250 of NFPA 70R-2023, although electrically it supplies a conductor with a dimension 12 times smaller. When there is an excess of sulphation of the conductors, the ground connection is inefficient, causing potential risks, mainly stored electrostatic charges.

Declaration of Competing Interest

The authors declare that they have no known competing financial interests or personal relationships that could have appeared to influence the work reported in this paper.

CRedit authorship contribution statement

Henry Pacheco: Methodology, Software, Formal analysis, Investigation, Writing. **Roger Salvatierra:** Methodology, Software, Formal analysis, Investigation, Writing. **Hernan Guillen:** Conceptualization, Methodology, Software, Formal analysis, Investigation, Writing - original draft, Writing - review & editing, Visualization.

Acknowledgments

Smart Grid Research Group (GIREI) of Salesian Polytechnic University (Project: ICT for Education) and the Power Grids and Smart Cities (RECI).

References

- [1] Abdaldaim, M., Wang, P., Li, L., 2017. The design of 110kv substation grounding grid with high resistivity soil, in: 2017 Sixth Asia-Pacific Conference on Antennas and Propagation (APCAP), pp. 1–3. doi:10.1109/APCAP.2017.8420847.
- [2] Amin, F., Rasel, M., Islam, S., 2021. Modeling and performance analysis of grounding system of a grid substation, in: 2021 International Conference on Science Contemporary Technologies (ICSCT), pp. 1–6. doi:10.1109/ICSCT53883.2021.9642701.
- [3] Anggoro, B., Utami, R.S., Handayani, L., 2019. Optimal design of grounding system substation, case study : 275/150 kv sigli substation, in: 2019 2nd International Conference on High Voltage Engineering and Power Systems (ICHVEPS), pp. 1–6. doi:10.1109/ICHVEPS47643.2019.9011064.
- [4] Barbecho Jimbo, J.F., Pérez Quiñónez, C.A., 2022. Propuesta para optimización sistemas de malla de puesta a tierra de las áreas de producción de UCEM-Planta Guapán. B.S. thesis.
- [5] Bonda, P.R., Mishra, M.K., 2018. Optimized design of earthing system for substations with high soil resistivity and limited plot area, in: 2018 20th National Power Systems Conference (NPSC), pp. 1–6. doi:10.1109/NPSC.2018.8771780.
- [6] Chen, L., Huang, K., Wei, K., Gao, D., Peng, Q., Lin, S., 2022. Study on the potential distribution characteristics of substation grounding grid considering stray current, in: 2022 IEEE 6th Conference on Energy Internet and Energy System Integration (EI2), pp. 1284–1289. doi:10.1109/EI256261.2022.10116337.
- [7] Desai, P., Unde, M., 2022. Cost-effective substation grounding design by unequally spaced grid conductors, in: 2022 1st International Conference on Sustainable Technology for Power and Energy Systems (STPES), pp. 1–5. doi:10.1109/STPES54845.2022.10006630.
- [8] Gargoom, A., Oo, A., Haque, M.E., Cavanaugh, M., Bernardo, J., 2018. Effect of substation grounding on the neutral voltage in substations with multiple independent resonant grounding systems, in: 2018 IEEE Industry Applications Society Annual Meeting (IAS), pp. 1–7. doi:10.1109/IAS.2018.8544597.
- [9] Hannig, M., 2018. Calculation of the assembled grounding resistance from complex grounding systems by using analytical considerations only, in: 2018 IEEE International Conference on High Voltage Engineering and Application (ICHVE), pp. 1–4. doi:10.1109/ICHVE.2018.8641921.
- [10] Hardi, S., Nasution, A., Fahmi, F., Purnamasari, F., 2020. Efficient design on the substation grounding grid: A case study at 2x500mva galang, in: 2020 4rd International Conference on Electrical, Telecommunication and Computer Engineering (ELTICOM), pp. 180–185. doi:10.1109/ELTICOM50775.2020.9230492.
- [11] IEEE, 2012a. Ieee guide for measuring earth resistivity, ground impedance, and earth surface potentials of a grounding system. IEEE Std 81-2012 (Revision of IEEE Std 81-1983) , 1–86doi:10.1109/IEEESTD.2012.6392181.
- [12] IEEE, 2012b. Ieee guide for temporary protective grounding systems used in substations. IEEE Std 1246-2011 (Revision of IEEE Std 1246-2002) , 1–69doi:10.1109/IEEESTD.2012.6143971.
- [13] IEEE, 2014. Ieee standard for qualifying permanent connections used in substation grounding. IEEE Std 837-2014 (Revision of IEEE Std 837-2002) , 1–59doi:10.1109/IEEESTD.2014.6922156.
- [14] IEEE, 2015. Ieee guide for safety in ac substation grounding. IEEE Std 80-2013 (Revision of IEEE Std 80-2000/ Incorporates IEEE Std 80-2013/Cor 1-2015) , 1–226doi:10.1109/IEEESTD.2015.7109078.
- [15] Kasim, I., Abduh, S., Fitriyah, N., 2017. Grounding system design optimization on 275 kv betung substation based on ieee standard 80-2000, in: 2017 15th International Conference on Quality in Research (QiR) : International Symposium on Electrical and Computer Engineering, pp. 400–407. doi:10.1109/QIR.2017.8168519.
- [16] Kumar, A., Kumar, V., Ashok, P.A., 2018. Unequally spaced grounding grid designed from equally spaced grounding grid for 220/132 kv substation, in: 2018 International Conference On Advances in Communication and Computing Technology (ICACCT), pp. 114–116. doi:10.1109/ICACCT.2018.8529430.
- [17] Liu, Z., Wang, S., Zhang, B., Cao, Y., Luo, D., Li, W., 2020. Method for reducing impulse grounding impedance of grounding device by using grounding electrode with non-uniform radius, in: 2020 IEEE International Conference on High Voltage Engineering and Application (ICHVE), pp. 1–4. doi:10.1109/ICHVE49031.2020.9279521.
- [18] Meng, Y., Chen, W., Liu, C., Luo, X., Huang, X., Tan, H., 2019. Influence of grounding design around down lead on lightning impulse behavior of substation grounding grid, in: 2019 11th Asia-Pacific International Conference on Lightning (APL), pp. 1–4. doi:10.1109/APL.2019.8816049.
- [19] Neamt, L., Balan, H., Chiver, O., Hotea, A., 2019. Considerations about substation grounding system design, in: 2019 8th International Conference on Modern Power Systems (MPS), pp. 1–4. doi:10.1109/MPS.2019.8759737.
- [20] Neamt, L., Chiver, O., 2021. A simple design method of unequal spacing arrangement for substation grounding grid. IEEE Access 9, 141339–141346. doi:10.1109/ACCESS.2021.3119941.
- [21] Oowaku, T., Inoue, Y., Najajima, M., Yamamoto, Y., Hayashiya, H., Yoshida, M., Matsumoto, A., Yasui, S., Ikeda, T., Mitome, H., Morita, G., 2018. Experimental study on surge response of grounding system of traction substation, in: 2018 34th International Conference on Lightning Protection (ICLP), pp. 1–6. doi:10.1109/ICLP.2018.8503499.
- [22] Owaku, T., Nakao, Y., Ikeda, T., Ookubo, M., Mitome, H., Hayashiya, H., 2019. Influence of grounding wire configuration of traction substation, in: 2019 11th Asia-Pacific International Conference on Lightning (APL), pp. 1–4. doi:10.1109/APL.2019.8816023.
- [23] Patel, A.B., Velani, K., 2017. Digital application for grounding grid design calculations of substation, in: 2017 Innovations in Power and Advanced Computing Technologies (i-PACT), pp. 1–6. doi:10.1109/IPACT.2017.8244947.
- [24] Ramli, S.S.M., Rosli, N.D.S., Ishak, N.H., Jamaludin, N.F., Omar, A.M.S., Ahmad, N.D., 2021. Development of apps software for designing high voltage ac substation grounding system with different shapes of grid with or without rods, in: 2021 6th IEEE International Conference on Recent Advances and Innovations in Engineering (ICRAIE), pp. 1–6. doi:10.1109/ICRAIE52900.2021.9704000.
- [25] S, F.M.S., P, F.A.Q., C, H.P.G., N, S.N.Q., 2018. Soil treatment to reduce grounding resistance by applying low-resistivity material (Irm) and chemical ground electrode in different grounding systems configurations, in: 2018 IEEE International Autumn Meeting on Power, Electronics and Computing (ROPEC), pp. 1–6. doi:10.1109/ROPEC.2018.8661403.

- [26] da Silva, L.N., Djambolakdjian, G.S., da Silva Gazzana, D., Ferraz, R.G., Vidor, F.F., 2022. Underground substation grounding evaluation using the average potential method, in: 2022 IEEE International Conference on Environment and Electrical Engineering and 2022 IEEE Industrial and Commercial Power Systems Europe (EEEIC / ICPS Europe), pp. 1–5. doi:10.1109/EEEIC/ICPSEurope54979.2022.9854572.
- [27] Siregar, Y., Hutaaruk, Y., Sinulingga, E., Suherman, 2021. Grounding systems in high voltage substation by analysis optimization design (case study : 150kv tapak tuan substation), in: 2021 5th International Conference on Electrical, Telecommunication and Computer Engineering (ELTICOM), pp. 64–68. doi:10.1109/ELTICOM53303.2021.9590117.
- [28] Wen, C., Quan, J., Li, X., Burean, W., Lin, H., Liu, H., Zhang, Z., Zhu, X., 2022. Optimization analysis of 220kv substation grounding network based on cdegs, in: 2022 IEEE 5th International Electrical and Energy Conference (CIEEC), pp. 4472–4476. doi:10.1109/CIEEC54735.2022.9846815.
- [29] Xuming, W., Ning, L., Qiaoyun, Z., Hang, L., Feng, Z., Shengnan, H., Menglu, C., 2022. Analysis of safety index in substation considering the damage of external ground network, in: 2022 IEEE 6th Conference on Energy Internet and Energy System Integration (EI2), pp. 658–663. doi:10.1109/EI256261.2022.10116108.
- [30] Yasui, S., Yamamoto, Y., Nakao, Y., Kobayashi, S., Ogihara, M., Hayashiya, H., 2018. Analytical study on improvement of traction substation's grounding system for lightning overvoltage reduction, in: 2018 34th International Conference on Lightning Protection (ICLP), pp. 1–6. doi:10.1109/ICLP.2018.8503291.
- [31] Zhou, L., He, J., Xu, H., Wang, P., Chen, Y., Chen, S., 2017. Simulation of impact of vertical grounding electrode on impulse grounding resistance of substation grounding network, in: 2017 2nd IEEE International Conference on Integrated Circuits and Microsystems (ICICM), pp. 18–22. doi:10.1109/ICAM.2017.8242130.